

Smart Cement Modified with Laponite for Real Time Monitoring of Oil Well Cementing Applications

C. Vipulanandan and A. Mohammed, Center for Innovative Grouting Materials and Technology (CIGMAT) and Texas Hurricane Center for Innovative Technology (THC-IT) - University of Houston.

Copyright 2017, AADE

This paper was prepared for presentation at the 2017 AADE National Technical Conference and Exhibition held at the Hilton Houston North Hotel, Houston, Texas, April 11-12, 2017. This conference is sponsored by the American Association of Drilling Engineers. The information presented in this paper does not reflect any position, claim or endorsement made or implied by the American Association of Drilling Engineers, their officers or members. Questions concerning the content of this paper should be directed to the individual(s) listed as author(s) of this work.

Abstract

Past three decades of oil well failures in the offshore facilities in the United States has clearly identified cementing to be the major cause of failures. In the year 2010, there was a major failure in the Gulf of Mexico and cementing has been identified as the cause of the failure. In the recent past, smart cement with very high sensing property has been developed for oil well applications. Also, clay materials are added to the cement to control the curing process, minimize the fluid loss, enhance the thermal properties and make the cement less brittle.

In this study, the effects of adding a nano clay material Laponite to the smart oil well cement (class H) with better sensing properties was investigated. Series of experiments evaluated the behavior of the smart cement with up to 1% Laponite (LP). Tests were performed on the smart cement from the time of mixing to the hardened state behavior. During the initial setting the electrical resistivity changed with time based on the amount of LP added to modify the smart oil well cement. The test results showed that the addition of LP increased the initial electrical resistivity of the cement slurries based on the amount of LP. The addition of LP up to 1% also affected the rheological properties, setting characteristics, and the piezoresistive properties of the smart cement. In a 24-hour period the maximum change in the electrical resistivity (RI_{24}) for the smart cement without LP (0.38 water-to-cement (w/c) ratio) was 333%. The RI_{24} for the cement with LP varied with the amount of LP. Addition of 1% LP increased the compressive strength. The smart cement was piezoresistive with the addition of LP but the sensitivity was decreased.

The shear thinning behavior of the smart cement slurries with and without LP at two temperatures have been quantified using the new Vipulanandan rheological model and compared it with the three material parameter, Vocadlo model. Based on the Vipulanandan rheological model the maximum shear tolerance with the smart cement without and with 1% LP at temperature of 25°C were 186 Pa and 404 Pa respectively, a 117 % increase. The smart cement modified with 1% of LP also affected the cement curing behavior and the piezoresistive behavior. Vipulanandan p-q curing model was used to predict the resistivity changes with curing time for the smart cement.

For the smart cement modified with LP, the resistivity change at peak stress was about 1000 times higher than the change in the compressive strain after 28 days of curing. Also, the addition of 1% LP increased the compressive strength by 46% after 28 days of curing.

Introduction

The oil and gas production is expanding around the world, but still there are unique challenges in well construction beginning at the seafloor. Preventing the loss of fluids to the formations and proper well cementing have become critical issues in well construction to ensure wellbore integrity because of varying downhole conditions (Ravi et al., 2007; Eoff et al., 2009; Labibzadeh et al., 2010). Moreover, the environmental friendliness of the cements and real time monitoring are critical issues that is oil well cement serves many purposes in the deep water drilling projects (Vipulanandan et al., 2014). Foremost important among these is to form a sealing layer between the well casing and the geological formation, referred to as the zonal isolation. With some of the reported failures and growing interest in addressing the environmental and economic concerns in the oil and gas industry, integrity of the cement sheath is of major importance. Recent case studies on cementing failures have clearly identified several issues that resulted in various types of delays in the cementing operations. Also preventing the loss of fluids to the formations and proper well cementing have become critical issues in well construction to ensure wellbore integrity because of varying down hole conditions (Eoff et al. 2009, Labibzadeh et al. , 2010 and Vipulanandan et al., 2015). The catastrophic accident in the Gulf of Mexico in April 2010 is one of the world's worst oil spills (Shadravan et al., 2012). The explosion at the drilling rig, Deepwater Horizon at Macondo claimed eleven lives and caused severe injuries to many others and record-breaking sea pollution from the release of about five million barrels of crude oil (Cristou et al., 2012). Two studies done by the Mineral Management Services (MMS) in the U.S. about the offshore oil well failures during the period of 1971 to 1991 and 1992 to 2006 clearly identified cement failures as the major cause for blowouts. Cementing failures increased significantly during the second period of

study when 18 of the 39 blowouts were due to cementing problem (Izon et al., 2007). With some of the reported failures and growing interest in environmental and economic concerns in the oil and gas industry, integrity of the cement sheath is of major importance. Therefore, proper monitoring and tracking the entire process of well cement become important to ensure cement integrity during the service life of the well (Vipulanandan et al., 2014).

For different types of cement applications additives such as clay, bentonite, silica fume, cement kiln dust and metakaolin to enhance the compression and bending strengths of the cement have been studied (Ata and Vipulanandan 1998; Celik et al. 2015). The use of clay as a partial cement replacement material up to 30% in mortar and concrete leads to improvement in the pore structure and high resistance to the transportation of water, the aggressive action of organic acids and diffusion of harmful ions which lead to degradation of the matrix (Li et al. 2003; Rashad 2015).

Electrical resistivity measurement has been applied by many researchers on concrete and cement applications (McCarter et al., 2006), but there are very limited information in the literature about the electrical resistivity measurements for characterizing oil well cement (Vipulanandan et al., 2015). Electrical response characteristics measurement has appropriate sensitivity in monitoring the characteristics of cementitious materials (McCarter et al., 1996). The advantages in using this technique include its accuracy, easy test procedure, and nondestructive characteristics (Xiao et al., 2008). Additionally, this method can be used for monitoring the long term behavior of cement in practice. Electrical resistivity of cement is affected by a number of factors such as pore structure (continuity and tortuosity), pore solution composition, cementitious content, water-to-cement ratio, moisture content, and temperature (Polder et al., 2001). Moreover, electrical resistivity of cement is dramatically affected by the contamination, due to the resistivity contrast between cement and the contaminating substance. Vipulanandan et al., (2006 - 2015) have studied the change in electrical resistivity with applied stress referred to as piezoresistive behavior of modified cementations and polymer composites. The studies showed that the changes in resistivity with the applied stress were 30 to 2800 times higher than the strain in the materials. Hence, the change in resistivity has the potential to be used to determine the integrity of the materials.

Objectives

The overall objective of this study was to investigate the effect of up to 1% of Laponite (LP) on the modified smart cement (Class H) behavior. The properties of interest were curing, rheological properties, compressive strength, and piezoresistive behavior. The specific objectives were as follows:

- i. Investigate the effect of LP on the rheological properties of smart cement and quantify the behavior.

- ii. Investigate the changes in the electrical resistivity during curing time of the smart cement.
- iii. Quantify the compressive strength and piezoresistive behavior of the LP modified smart cement.

Materials and Methods

Smart Cement

Commercially available oil well cement (Class H cement) was modified with less than 0.1% additive to make it a piezoresistive material.

Laponite (LP)

Commercially available Laponite was used in this study. Based on the manufactures data the Laponite had 60% of SiO₂, 27.5% of MgO and 0.8% of Li₂O.

Methods

Cement Mixture

The samples were prepared according to the API standards. Smart cement with a w/c ratio of 0.38 was used in this study. Four batches of cement slurries without and with 1% of LP were prepared.

Cement Specimen Preparation

After mixing, cement specimens were prepared in the plastic cylindrical molds with a diameter of 2 inches and a height of 4 inches. Two conductive wires were placed in all of the molds which were 5 cm apart. All specimens were capped to minimize the moisture loss and were cured up to the 28 days for the piezoresistivity test under compressive loading.

Rheological Tests

Rheological properties determine the ability of cement to be pumped. The rheology tests were performed by utilizing a rotational viscometer at room pressure and temperature at rpms ranging from 3 to 600 rpm, and the shear stresses were recorded. The viscometers were calibrated using several standard solutions.

Electrical Resistivity

Two different instruments were used to measure the electrical resistivity of the smart cement.

(i) Conductivity Probe

Commercially available conductivity probe was used to measure the conductivity (inverse of electrical resistivity) of the cement slurry. The conductivity measuring range was from 0.1 μS/cm to 1000 mS/cm representing a resistivity of 100,000 Ω.m to 0.01 Ω.m.

(ii) Digital Resistivity Meter

Digital resistivity meter measured the resistivity of fluids, slurries and semi-solids with resistivity in the range of 0.01 Ω.m. to 400 Ω.m. Both of the electrical resistivity devices were calibrated using standard solution. Based on past studies, electrical resistivity was selected as the monitoring parameter

to quantify the performance of modified cement during curing and hardening process (Vipulanandan et al. 2013). Further, electrical resistance was measured using the LCR meter with the curing time. To minimize the contact resistances, the resistance was measured at 300 kHz using two-wire method (Vipulanandan et al. 2013). Each specimen was calibrated to obtain the electrical resistivity (ρ) from the measured electrical resistance (R) using Eqn.(1).

$$R = \rho * \left(\frac{L}{A}\right) = \rho K \quad (1)$$

where L is the distance between the wires, A is the cross-sectional area through which the current is flowing, and L/A is called the geometry factor. In addition to geometry, other interfacial factors are important in obtaining electrical resistivity from electrical resistance. Hence, L/A in Eqn.1 is replaced by an experimentally determined calibration factor (K), by measuring the resistivity (ρ) and resistance (R) of the cement slurry during the first three hours of curing. It has been shown that the parameter K reaches a very stable value during the first three hours of curing. Normalized change in resistivity with the changing conditions can be represented as follows:

$$\frac{\Delta\rho}{\rho} = \frac{\Delta R}{R} \quad (2)$$

In general total represent resistivity (ρ) is used to the composition and curing characteristics. The incremental resistivity ($\Delta\rho$) is used as a monitoring tool.

Compressive Strength Tests (ASTM C39)

Compressive strength of the cement determines the ability of cement to stabilize casing in the wellbore. The cylindrical specimens were capped and tested at a predetermined rate of displacement. Compression tests were performed on cement samples after 1 and 28 days of curing using a hydraulic compression machine.

Piezoresistivity Tests

Piezoresistivity describes the change in electrical resistivity of a material under stress. Since oil well cement serves as a pressure-bearing part of the wells in real applications, the piezoresistivity of smart cement with and without LP was investigated under compressive loading. During each compression test, electrical resistance was measured along the stress axis. To eliminate the polarization effect, alternating current (AC) resistance measurements were made using a LCR meter at a frequency of 300 kHz. Furthermore, changes in resistivity were related to the applied stress.

Results and Discussions Modelling

(i) Vocadlo model (1969)

Due to the shear-thinning behavior of the cement slurries

Bingham plastic model was not an accurate model to estimate the shear stress - shear strain rate relationship. The advantage of the proposed model is its higher accuracy especially at higher strain shear strain rates. A comparison of the proposed model with the Vocadlo model (Eqn. 3) which is being used in industry is shown in Fig. 1.

$$\tau = [\tau_{o1}^{\frac{1}{n}} + k^{\frac{1}{n}} * \dot{\gamma}^{0.5}]^{1/n} \quad (3)$$

when $\dot{\gamma} \rightarrow \infty \Rightarrow \tau_{max} = \infty$

(ii) Vipulanandan Rheological model (2014)

To predict the shear stress- shear strain rate relationship a Vipulanandan rheological model (2014) was proposed to predict the experimental data and the trend observed (Vipulanandan and Mohammed 2014). The developed Vipulanandan rheological model is represented in Eqn. (4) as follows:

$$\tau = \tau_{o2} + \frac{\dot{\gamma}}{A + \dot{\gamma}D} \quad (4)$$

where τ_{o2} is the yield stress at zero shear strain rate (Pa), $\dot{\gamma}$ is the shear strain rate (s^{-1}) and A and D are the hyperbolic model parameters. Experimental data and Vipulanandan rheological model prediction for the smart cement slurries are shown in Fig. 1. when

$$\dot{\gamma} \rightarrow \infty \Rightarrow \tau_{max} = \frac{1}{D} + \tau_o \quad (5)$$

Rheological properties

Smart cement slurries with w/c ratio of 0.38 at two different temperatures showed significantly different rheological properties. However, regardless of the LP percentage and temperature, all slurries exhibited non-Newtonian and shear-thinning behavior as shown in Fig. 1.

Rheological models

Shear stress–shear strain rate relationships were predicated using the Vipulanandan rheological model and compared with Vocadlo model (Fig. 1).

(i) Vocadlo model (1969)

(a) LP=0%

The shear thinning behavior of smart cement slurry with w/c ratio of 0.38 without LP at two different temperatures 25°C and 85°C were modeled using the Vocadlo model (Eqn. (3)) up to a shear strain rate of 1024 s^{-1} (600 rpm). The coefficient of determination (R^2) was greater than 0.97 as summarized in Table 1. The root mean square of error (RMSE) varied between 5.91 Pa and 11.1 Pa based on the temperature as summarized in Table 1. The yield stress (τ_{o1}) for the cement slurry at temperature of 25°C was 20.1 Pa, with increasing the temperature of the slurry to 85°C, the yield stress increased to 42.5 Pa, a 99.5% increase as summarized in

Table 1. The model parameter k for the cement slurry at temperatures of 25°C and 85°C varied between 21.3 Pa.sⁿ and 4.6 Pa.sⁿ respectively as summarized in Table 1. The model parameter n for the cement slurry decreased from 0.75 to 0.56 with the increase in the temperature to 85°C as summarized in Table 1.

(b) LP=1%

Using the Vocadlo model (Eqn. (3)), the relationships between shear stress with shear strain rate of for the smart cement slurry mud with 1% LP at 25°C and 85°C of temperature and with w/c ratio of 0.38 were modeled. The coefficient of determination (R²) varied between 0.98 and 0.99 as summarized in Table 1. The root mean square of error (RMSE) varied from 8.76 Pa to 13.93 Pa as summarized in Table 1. The yield stress (τ_{o1}) for the cement slurry at 25°C was 31.5 Pa and increased to 62.6 Pa with increasing the temperature to 85°C, a 98% increase as summarized in Table 1. The model parameter k for the cement slurry at 25°C and 85°C varied between 20.6 Pa.sⁿ and 69.3 Pa.sⁿ based on the temperature and LP content. The model parameter n for cement slurry decreased from 0.76 to 0.54 with increasing the temperature to 85°C as summarized in Table 1.

(ii) Vipulanandan Rheological Model (2014)

(a) LP=0%

The shear thinning behavior of the smart cement slurry with LP of 0% at 25°C and 85°C were modeled using the Vipulanandan rheological model (Eqn. (4)). The coefficient of determination (R²) was greater than or equal to 0.98 as summarized in Table 1. The root mean square of error (RMSE) varied between 5.7 Pa and 9.9 Pa respectively as summarized in Table 1. The yield stress (τ_{o2}) of the smart cement slurry at 25°C was 19.3 Pa and it increased to 53.2 Pa with increasing the temperature to 85°C, a 175% increase as summarized in Table 1. The model parameter A for the smart cement slurry at 25°C and 85°C varied between 1.62 Pa.s⁻¹ and 0.59 Pa.s⁻¹ respectively as summarized in Table 1. The model parameter D for the smart cement slurry at 25°C and 85°C was 0.006 Pa⁻¹ and 0.003 Pa⁻¹ respectively, as summarized in Table 1.

(b) LP=1%

Using the Vipulanandan rheological model (Eqn. (4)), the relationships between shear stress with shear strain rate of the smart cement slurry with 1% of LP at 25°C and 85°C were modeled. The coefficients of determination (R²) was greater than 0.98 as summarized in Table 1. The root mean square of error (RMSE) varied between 9.92 Pa and 14.1 Pa based on the temperature as summarized in Table 1. Additional of 1% LP to the cement slurry at 25°C increased the yield stress (τ_{o2}) to 33.7 Pa, an increase of 75% as summarized in Table 1. The model parameter A for the cement slurry at 25°C and 85°C varied between 1.03 Pa.s⁻¹ and 0.45 Pa.s⁻¹ as summarized in Table 1. The model parameter D at 25°C and 85°C were 0.003 Pa⁻¹ and 0.002 Pa⁻¹ respectively as summarized in Table 1.

Maximum Shear Stress (τ_{max})

Based on Eqn. 5 the Vipulanandan rheological model has a limit on the maximum shear stress the slurry will produce at relatively very high rate of shear strain. The τ_{max} for smart cement slurries with 0% and 1% of LP content at 25°C were 186 Pa and 404 Pa respectively as summarized in Table 1. Increasing the temperatures of the smart cement slurries to 85°C increased the maximum shear stress by 108% and 38% for smart cement modified using 0% and 1% of LP respectively as summarized in Table 1.

Electrical Resistivity

Based on the current study and past experience of the researchers, the change in resistivity with time can be represented as shown in Fig. 2. Hence several parameters can be used in monitoring the curing (hardening process) of the cement. The parameters are initial resistivity (ρ_o), minimum resistivity (ρ_{min}), time to reach the minimum resistivity (t_{min}), resistivity after 24 hours of curing (ρ₂₄) and percentage of maximum change in resistivity (Resistivity Index) [RI₂₄=($\frac{\rho_{24}-\rho_{min}}{\rho_{min}}$)*100]. The test results from various smart cement compositions are summarized in Table 2. The initial electrical resistivity (ρ_o) of smart cement with 0% and 1% of LP were 1.03 Ω.m and 1.24 Ω.m respectively, a 20% increase in the electrical resistivity when LP concentration was increased by 1%. Also the t_{min} was reduced by 36% when LP concentration increased by 1% as summarized in Table 2. The minimum resistivity (ρ_{min}) of smart cement with 0% and 1% of LP were 0.90 Ω.m and 1.09 Ω.m, a 21% increase in the electrical resistivity when LP concentration increased by 1%. The Resistivity index (RI_{24hr}) for smart cement with 0% and 1% of LP were 333% and 312% respectively as summarized in Table 2. These observed trends clearly indicate the sensitivity of resistivity to the changes occurring in the curing of cement (Table 2). Based on experimental results, Vipulanandan p-q model proposed by Vipulanandan and Paul (1990) was modified to predict the electrical resistivity of smart cement during hydration up to 7 days of curing a shown in Fig. 3. The Vipulanandan p-q Curing Model (2015 b) is defined as follows:

$$\frac{1}{\rho} = \left(\frac{1}{\rho_{min}}\right) \left[\frac{\left(\frac{t+t_o}{t_{min}+t_o}\right)}{q1+(1-p1-q1)*\left(\frac{t+t_o}{t_{min}+t_o}\right)+p1*\left(\frac{t+t_o}{t_{min}+t_o}\right)^{\frac{q1+p1}{p1}}} \right] \quad (6)$$

where:

ρ: electrical resistivity (Ω-m), ρ_{min}: minimum electrical resistivity (Ω-m), t_{min}: time corresponding minimum electrical resistivity (ρ_{min}), p1 = (A + B), to, A, B and q₁ are model parameters (Table 3) and t: time (min).

Compressive Strength

Effect of LP

1 day of curing

The compressive strength (σ_f) of the cement with w/c ratio of 0.38 modified with 0% and 1% of LP after 1 day of curing were 1583 psi and 2502 psi, a 58% increase as summarized in Table 4.

28 days of curing

The compressive strength (σ_f) of the cement with w/c ratio of 0.38 without and with 1% of LP after 28 days of curing were 2810 psi and 4101 psi, a 46% increase as summarized in Table 4.

Piezoresistivity Behavior of Smart Cement

The piezoresistive behavior of the smart cement was investigated with up to 1% LP.

1 day of curing

The piezoresistive behavior of the cement (no additive) is shown in Fig. 5. After 1 day of curing the piezoresistivity at failure for the cement with w/c ratio of 0.38 was 0.72% as summarized in Table 4. Additional of 0.1% CF to the cement with w/c ratio of 0.38 increased the change in electrical resistivity of oil well cement at failure ($\frac{\Delta\rho}{\rho_o}_f$) to 533% as summarized in Table 4. Additional of 1% of LP to the smart cement after 1 day of curing decreased the electrical resistivity at failure ($\frac{\Delta\rho}{\rho_o}_f$) to 296% as summarized in Table 4. The Piezoresistivity at failure with 1% LP addition was about 1500 times higher than the compressive strain at failure of 0.2%.

28 days of curing

The piezoresistivity at failure for the cement (no additive) with w/c ratio of 0.38 was 0.55% as summarized in Table 4. Additional of 0.1% CF to the cement with w/c ratio of 0.38 increased the change in electrical resistivity of oil well cement at failure ($\frac{\Delta\rho}{\rho_o}_f$) to 401% as summarized in Table 4. Addition of 1% of LP to the smart cement after 28 days of curing decreased the electrical resistivity at failure ($\frac{\Delta\rho}{\rho_o}_f$) from 401% to 211% as summarized in Table 4. The piezoresistivity at failure with 1% LP addition was over 1000 times higher than the compressive stain at failure.

Compressive Strength – Resistivity Relationship.

During the entire cement hydration process both the electrical resistivity and compressive strength of the cement increased gradually with the curing time. For cement pastes with various LP content, the change in resistivity was varied during the hardening. The cement paste without LP had the lowest electrical resistivity change (RI_{24hr}), as shown in Table 2.

The relationships between (RI_{24hr}) and the 1 day and 28 days cured cement compressive strengths (psi) (Fig. 6) were as

follows:

1 day of curing

$$\sigma_{1day} = 22803 - 60 \times RI_{24hr} \quad (7)$$

28 day of curing

$$\sigma_{28days} = 16016 - 43.3 \times RI_{24hr} \quad (8)$$

Conclusions

Based on this experimental and analytical study on smart cement with up to 1% Laponite (LP), the following conclusions are advanced:

1. The rheological test showed that class H cement had shear-thinning behavior and the new Vipulanandan rheological model predicted the shear stress-strain rate relationship very well.
2. Additional of Laponite increased the resistivity of the mix and also changed the curing pattern. Vipulanandan p-q curing model predicted the resistivity change with curing time very well.
3. The resistivity index (RI_{24hr}) of the cement with lower LP concentration was higher than that of the cement with higher LP concentration linear correlation was found between resistivity index and compressive strength at different curing ages.
4. Addition of LP reduced the piezoresistivity of smart cement at both curing ages investigated. The resistivity change at peak stress was over 1000 times higher than the change in compressive strain after 28 days of curing. Also, the addition of 1% LP increased the compressive strength by 46%.

Acknowledgements

This study was supported by the Center for Innovative Grouting Materials and Technology (CIGMAT) and Texas Hurricane Center for innovative Technology (THC-IT) at the University of Houston, Houston, Texas with funding from DOE/NETL/RPSEA (Project 10121-4501-01).

References

1. API Recommended Practice 10B (1997), Recommended Practice for Testing Well Cements Exploration and Production Department, 22nd Edition.
2. API Recommended Practice 65 (2002) Cementing Shallow Water Flow Zones in Deepwater Wells.
3. Ata, A., and Vipulanandan, C. (1997). Silica fume in Silicate and Cement Grouts and Grouted Sands. Geotechnical Special Publication, 242-257.
4. Celik, F., and Canakci, H. (2015). An investigation of rheological properties of cement-based grout mixed with rice husk ash (RHA). Construction and Building Materials, 91, 187-194.

5. Cristou, M., and Konstantinidou, M., (2012) "Safety of offshore oil and gas operations: Lessons from past accident analysis." Joint Research Centre of the European Commission, pp. 1-60.
6. Eoff, L. and Waltman, B. (2009) "Polymer Treatment Controls Fluid Loss While Maintaining Hydrocarbon Flow," *Journal of Petroleum Technology*, pp. 28-30.
7. Izon, D. and Mayes, M., (2007) "Absence of fatalities in blowouts encouraging in MMS study of OCS incidents 1992-2006" *Well Control*, pp. 86-90.
8. Labibzadeh, M., Zhabizadeh, B., and Khajehdezfuly, A. (2010) "Early Age Compressive Strength Assessment of Oil Well Class G Cement Due to Borehole Pressure and Temperature Changes," *Journal of American Science*, Vol. 6, No.7, pp.38-47.
9. McCarter, W. J. (1996) "Monitoring the influence of water and ionic ingress on cover-zone concrete subjected to repeated absorption", *Cement Concrete and Aggregates*, 18, pp. 55-63.
10. Mohammed, S. (2016). Effect of temperature on the rheological properties with shear stress limit of iron oxide nanoparticle modified bentonite drilling muds. *Egyptian Journal of Petroleum*, 10.1016/j.ejpe.2016.10.018.
11. Polder, R.B., (2001) "Test Methods for on Site Measurements of Resistivity of Concrete-a RILEM TC-154 Technical Recommendation," *Construction and Building Materials*, Vol. 15.
12. Rashad, A. M. (2015). Metakaolin: fresh properties and optimum content for mechanical strength in a comprehensive overview. *Rev. Adv. Mater. Sci*, 40, 15-44.
13. Ravi, K. et al. (2007) "Comparative Study of mechanical Properties of Density-reduced Cement Compositions," *SPE Drilling & Completion*, Vol. 22, No. 2, pp. 119-126.
14. Shadravan, A. and Amani, (2012) "M HPHT 101- What petroleum engineers and geoscientists should know about high pressure high temperature wells." *environment Journal of Energy Science and Technology*, pp.36-60.
15. Vipulanandan, C., and Paul, E. (1990). Performance of epoxy and polyester polymer concrete. *Materials Journal*, 87(3), 241-251.
16. Vipulanandan, C., and Garas, V. (2006), "Piezoresistivity of Carbon Fiber Reinforced Cement Mortar", *Proceedings, Engineering, Construction and Operations in Challenging Environments*," *Earth & Space 2006, Proceedings ASCE Aerospace Division*, League City, TX, CD-ROM.
17. Vipulanandan, C. and Garas, V. (2008) "Electrical Resistivity, Pulse Velocity and Compressive Properties of Carbon Fiber Reinforced Cement Mortar," *Journal of Materials in Civil Engineering*, Vol. 20, No. 2 , pp. 93-101.
18. Vipulanandan, C. and Prashanth, P. (2013) "Impedance Spectroscopy Characterization of a Piezoresistive Structural Polymer Composite Bulk Sensor," *Journal of Testing and Evaluation*, ASTM, Vol. 41, No. 6, pp. 898-904.
19. Vipulanandan, C. and A. Mohammed, (2014a) "Hyperbolic rheological model with shear stress limit for acrylamide polymer modified bentonite drilling muds", *Petroleum Science and Engineering*, 122, pp. 38-47.
20. Vipulanandan, C., Heidari, M., Qu, Q., Farzam, H. and Pappas, M. (2014b). "Behavior of Piezoresistive Smart Cement Contaminated with Oil Based Drilling Mud." *OTC 25200-MS*, pp. 1-14.
21. Vipulanandan, C., Mohammed, A. and Qu, Q. (2014c)."Characterizing the Hydraulic Fracturing Fluid Modified with Nano Silica Proppant." *AADE-14-FTCE-39*, pp. 1-12.
22. Vipulanandan, C., and Amani, N. (2015a). Behavior of Nano Calcium Carbonate Modified Smart Cement Contaminated with Oil Based Drilling Mud. *In Offshore Technology Conference. Offshore Technology Conference*.
23. Vipulanandan, C., and Mohammed, A. (2015 b). Smart cement rheological and piezoresistive behavior for oil well applications. *Journal of Petroleum Science and Engineering*, 135, 50-58.
24. Vipulanandan, C., and Mohammed, A. (2015 c). Smart cement modified with iron oxide nanoparticles to enhance the piezoresistive behavior and compressive strength for oil well applications. *Smart Materials and Structures*, 24(12), 125020.
25. Xiao, L., and Li, Z. (2008). "Early-Age Hydration of Fresh Concrete Monitored by Non-contact Electrical Resistivity Measurement." *Cement and Concrete Research*, 38(3), 312-319.

Table 1. Vocadlo and Vipulanandan rheological model parameters for smart cement slurries

LP (%)	T (°C)	Vocadlo Model (1969)					Vipulanandan Rheological Model (2014)					
		τ_{o1} (Pa)	k (Pa.s ⁿ)	n	RMSE (Pa)	R ²	τ_{o2} (Pa)	A (Pa.s ⁻¹)	D (Pa) ⁻¹	τ_{max} (Pa)	RMSE (Pa)	R ²
0	25	20.1	21.3	0.75	5.91	0.98	19.3	1.62	0.006	186	5.7	0.98
	85	42.5	4.6	0.56	11.1	0.98	53.2	0.59	0.003	387	9.9	0.99
0.5	25	24.8	13.6	0.79	4.94	0.99	24.0	1.52	0.004	274	4.88	0.99
	85	45.4	48.5	0.59	13.38	0.98	49.1	0.39	0.003	449	10.30	0.98
1	25	31.5	20.6	0.76	8.76	0.98	33.7	1.03	0.003	404	9.92	0.99
	85	62.6	69.3	0.54	13.93	0.99	60.3	0.45	0.002	560	14.1	0.99

Table 2. Summary of bulk resistivity parameters for cement with various Laponite (LP) content

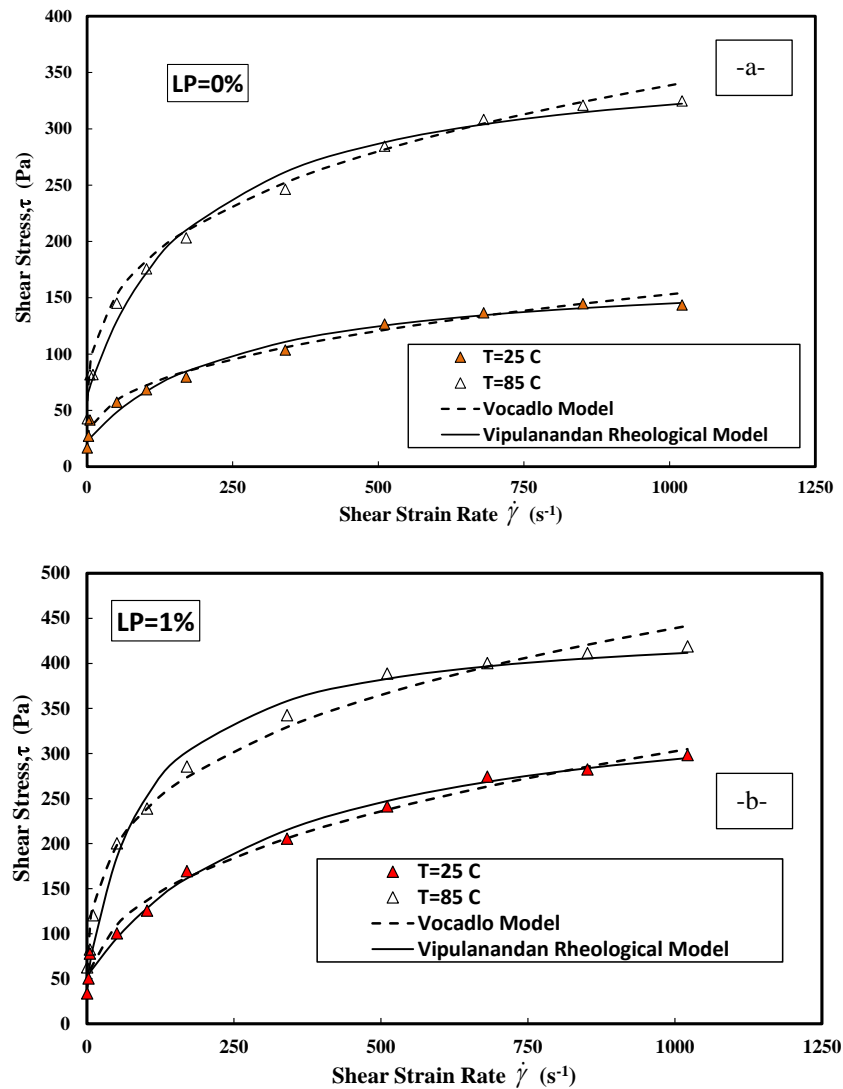
LP (%)	Initial resistivity, ρ_o ($\Omega.m$)	ρ_{min} ($\Omega.m$)	t_{min} (min)	ρ_{24hr} ($\Omega.m$)	RI _{24 hr} (%)
0	1.03	0.90	163	3.90	333
0.5	1.10	1.02	125	4.04	320
1	1.24	1.09	105	4.50	312

Table 3. Model parameters for electrical resistivity of smart cement with different Laponite (LP) content

LP (%)	Curing Time (day)	ρ_{min} ($\Omega.m$)	t_{min} (min)	q_1	t_o (min)	A	B	R ²
0	1	0.90	168	1.60	130	-0.0001	7.23	0.99
	7			2.20	75	-0.0001	18.8	0.99
0.5	1	1.10	125	1.89	125	-0.0001	10.5	0.99
	7			2.32	70	-0.0001	33	0.99
1	1	1.24	105	3.56	95	-0.0001	23.3	0.99
	7			4.19	228	-0.0001	36	0.99

Table 4. Variation of piezoresistive behavior for cement with different Laponite (LP) content

Material	LP (%)	Curing Time (day)	$(\Delta\rho/\rho_0)_f$ (%)	σ_f (psi)
Cement only	0	1	0.72	1544
		28	0.55	2504
Smart cement	0	1	533	1583
		28	401	2810
	1	1	296	2502
		28	211.4	4101

**Figure 1. Predicted and measured shear stress-shear strain rate relationship for smart cement slurries with different Laponite (LP) content and different temperature (a) LP=0% and (b) LP=1%**

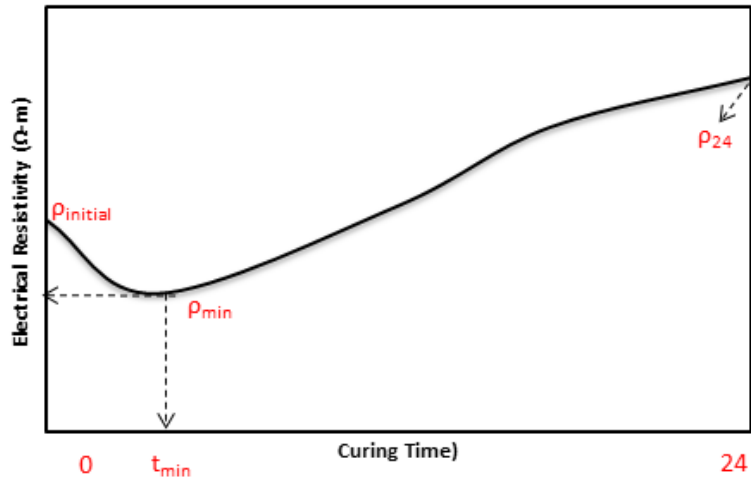


Figure 2. Typical bulk resistivity development with curing time

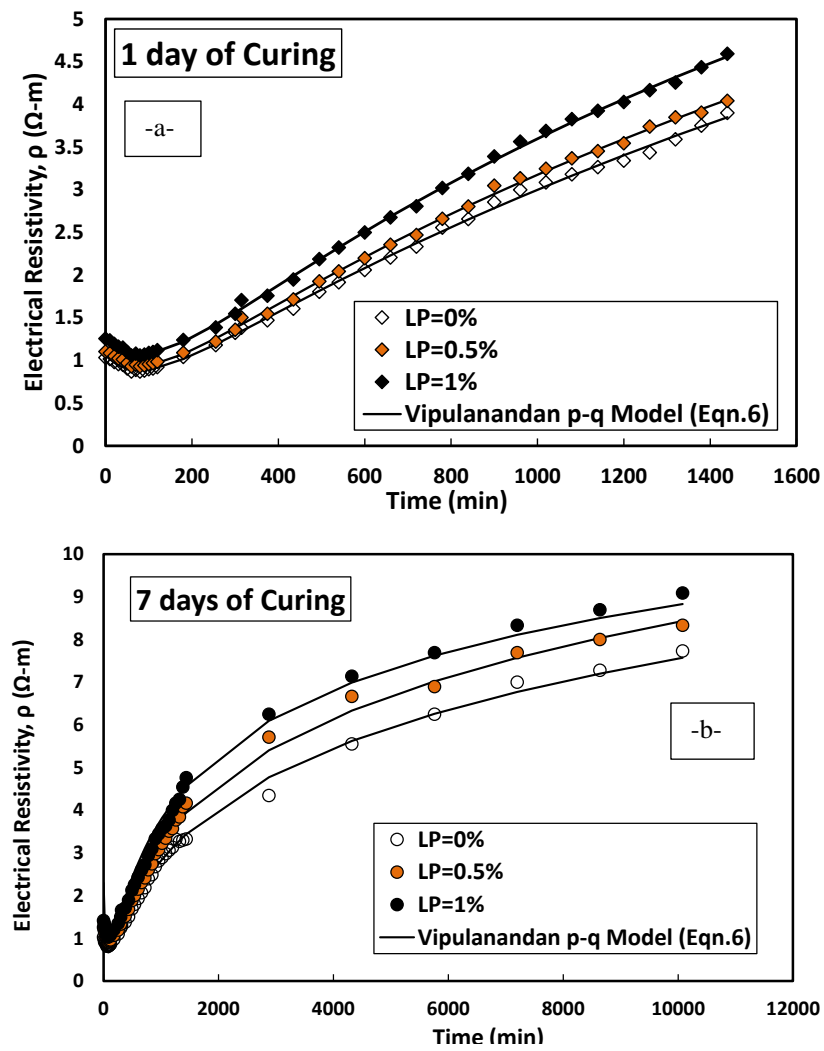


Figure 3. Bulk electrical resistivity development of smart cement modified with different Laponite (LP) content (a) 1 day of curing and (b) 7 days of curing

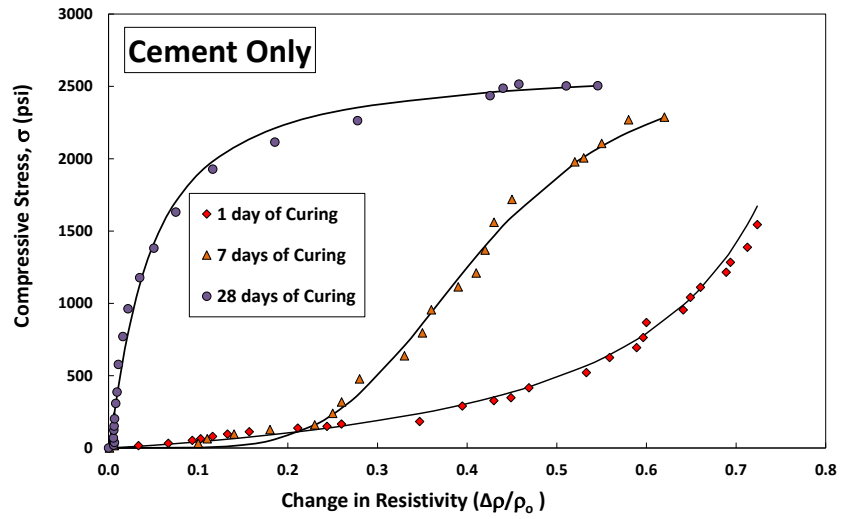
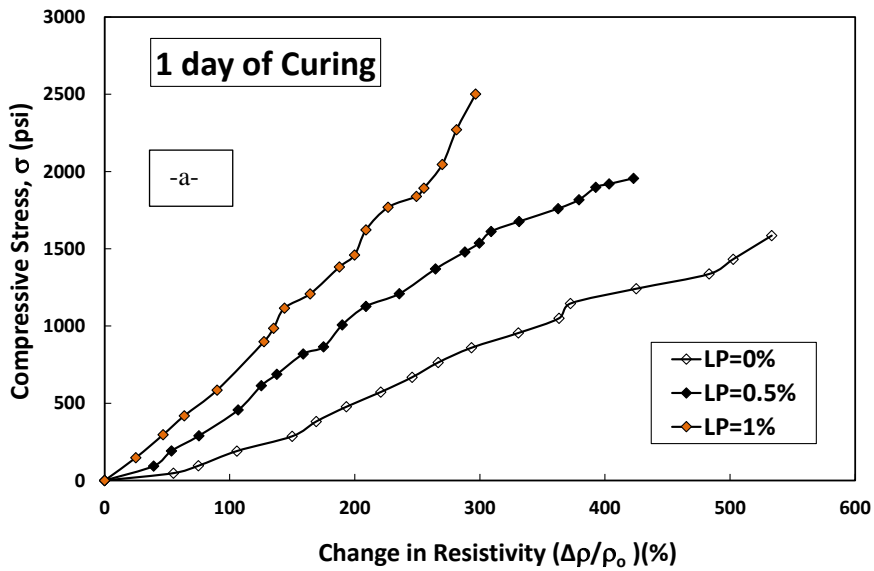


Figure 4. Piezoresistive behaviour of oil well cement with different curing time



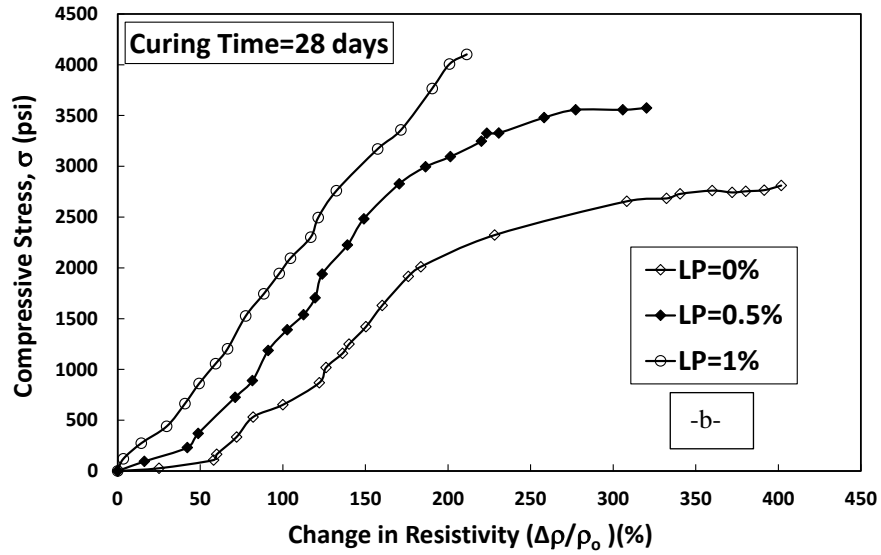


Figure 5. Piezoresistive behaviour of smart oil well cement with different Laponite (LP) content at (a) 1 day of curing and (b) 28 days of curing

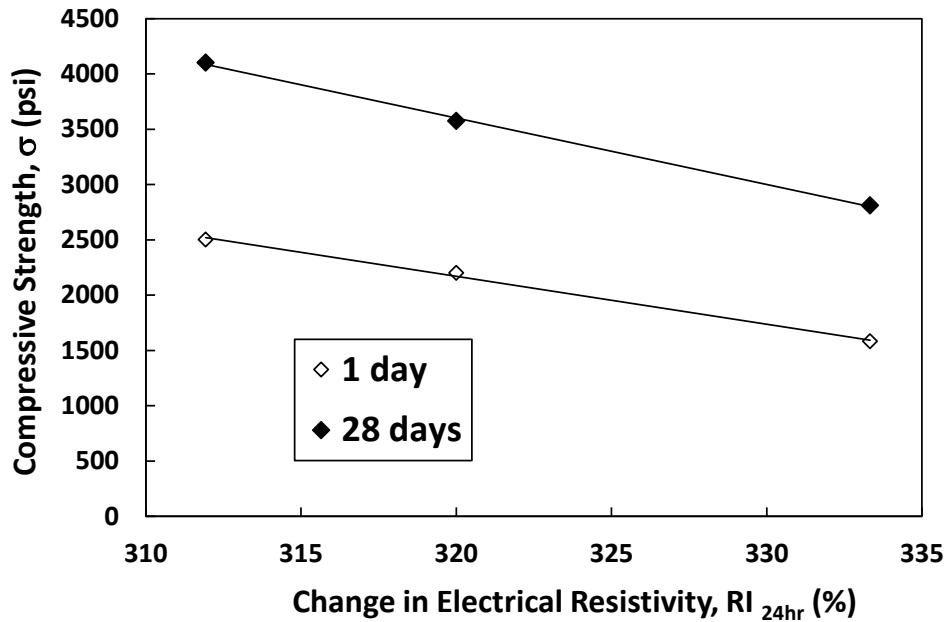


Figure 6. Relationship between resistivity index (RI_{24hr}) and compressive strength of smart cement modified with Laponite (LP)